95-GT-421

BLADING VIBRATION AND FAILURES IN GAS TURBINES PART D: CASE STUDIES

Cyrus B. Meher-Homji
Boyce Engineering International, Inc.
10555 Rockley Road,
Houston, Texas.

ABSTRACT

The investigation of gas turbine blade failures requires an interdisciplinary approach calling for expertise in gas turbine design, operation and metallurgy. The object of this paper is to show, in the context of blading problems, the *interrelationship* between design, operation, maintenance, and the operational envelope. This paper presents case studies dealing with a variety of failure modes. The treatment focuses on practical troubleshooting of blading problems augmented, in some cases, by the use of analytical tools.

1.0 INTRODUCTION

With blades accounting for as high as forty two percent (42%) of the failures in gas turbines (Allianz, 1978) and with its severe effect on plant availability, there is a pressing need for a unified treatment of the causes, failure modes and troubleshooting to assist plant engineers in tackling blade failure problems. Existing publications tend to focus exclusively on a particular aspect of the problem such as metallurgy, vibration dynamics or design or stress analysis and fail to emphasize the multidisciplinary nature of the problem. Some notable exceptions are publications by Dundas(1993a,b), Sohre (1975) Passey(1976) and Armstrong (1960) which provide a practical perspective. It is the intent of this paper along with Meher-Homji, (1995 A,B,C) to provide a practical, treatment to aid gas turbine users tackle blading problems.

When a catastrophic blade failure occurs in a critical gas turbine, there is considerable pressure to get the machine operational expeditiously. Strategies followed to resolve the problem may involve design changes, and at times, alteration of the turbine's operational envelope. The strategy chosen is dependent on the failure mode and the root cause. In certain situations, it may be imperative that the machine be kept operational due to economic constraints in spite of obvious mechanical distress. In such circumstances, monitoring of performance and other parameters as delineated in Meher-Homji (1995c) may be of value as it allows adjustment of the operational envelope to avoid dangerous regimes till a convenient outage can be taken.

The troubleshooting of blade failures involves:

1. Examination of the evidence. This should include not only the failed components but also the gas turbine operational and maintenance environment, log sheet data, and history. Frequently, troubleshooters plunge into detailed analytical studies without paying attention to practical observations.
2. Development of hypotheses as to the root cause of the failure.
3. Reconciling the evidence with the hypotheses ensuring that it fits the hypothesized scenario. If the evidence does not fit, the hypothesis has to be modified. This step may encompass metallurgical and analytical studies.
4. Development of short and long term solution strategies. Short term strategies could involve changing the operational envelope[1] and close monitoring of operational parameters. Long term solutions may include redesign or strengthening of the blade, reduction of stimuli which excite vibration or instituting rigid quality control measures to check dimensional accuracy, finishes and coating quality.

In the case studies presented ahead, dates and other data have been modified in order to keep the user and OEM anonymous. The technical essence of the cases have, however, been maintained.

2.0 HOT SECTION BLADING FAILURE OF A LARGE UTILITY GAS TURBINE

2.1 Background.

The gas turbine generator under consideration was site rated at 100 MW and operated on distillate fuel. The turbine was inspected 3 months prior to the failure. During this inspection, corrosion and deposits were found on the hot section and a decision was made to allow the gas turbine to continue operation to 24,000 equivalent hours before an overhaul outage. The gas turbine was a well proven and reliable design utilizing silo type combustors, operating at a turbine inlet temperature of 1050°C (1922 °F) an air mass flow rate of 1056 Lb/sec (480 Kg/sec) and a pressure ratio of 10:1. It had a 16 stage axial flow compressor and a 4 stage turbine.

On the day of the failure, the turbine tripped on excessive vibration while running at a load of 115 MW. The turbine had

[1] This could involve changing speed, power, imposing temperature restrictions, better environmental control or minimizing starts and stops.

Presented at the International Gas Turbine and Aeroengine Congress and Exposition
Houston, Texas - June 5-8, 1995

undergone 473 starts and had 8,900 actual operating hours. Upon dismantling the turbine, thirty 1st stage turbine blades were found severely damaged. Subsequent DOD had wrecked the other stages. Parts of a fire brick from the top of the right side combustion chamber were found lying in the stationary nozzle vanes located at the 6 O'clock position. Another piece was found at the center bottom of the inner casing.

2.2 Investigation.

The investigation conducted, encompassed a detailed review of the failed turbine, metallurgical analyses, and the historical log sheets which were analyzed for performance data and trends. Special emphasis was placed on evaluation of exhaust gas temperature (EGT) profiles and spreads.

2.3 Metallurgical Findings.

After examination of the debris, components including the 1st stage rotor blades, 2nd stage blades, and sections of the 1st stage nozzle were selected for metallurgical analysis. The conclusions of the metallurgical study were:

1) The fracture surface of a particular 1st stage blade indicated fatigue.
2) Blade material was confirmed to be IN 738 with chrome diffusion coatings
3) There was evidence of sulphidation.
4) There was no evidence of over temperature.

The observation that the aft portion of the fracture surface on a first stage blade was caused by fatigue, suggested that a fatigue mechanism was present. Observations of the Trailing Edge (TE) region of another 1st stage blade, indicated that hot corrosion damage had reduced the pressure side wall of the lowest cooling hole to an extreme thinness. This, in conjunction with the fact that the plane of maximum bending stress coincided with this hole, explained the nucleation and propagation of a fatigue crack. Photographs shown in Figure 1 depict the failure.

2.4 Situation Analysis

Some observations pertaining to the failed unit and an identical unit operating at the same site were:

(1) Analysis of the vibration data of the failed machine (log sheets and strip charts) indicated that there was no progressive growth in overall vibration levels over time. The absolute vibration levels were acceptable.
(2) Examination of the nozzle section of the operational turbine indicated the presence of salts. This was clear evidence that salt ingestion had taken place. As the fuel treatment system was performing effectively, the salt must have been airborne[2].
(3) Figure 2 shows a sketch of the section of the brick that was found lodged in the 6 O'clock position of the nozzle accounting for a blockage of about 80% of that vane space. This was a significant contributing factor to the failure as blockage of this nature produced damaging vibratory stresses on the rotating blades, by disrupting airflow.

2.4.1 Data Log Sheet Analysis. Extensive analyses of the "4 hour" log sheets were conducted. Calculations and trends were made of the corrected speed, power , pressure ratio, thermal efficiency, compressor efficiency , compressor intake depression and calculated Turbine Inlet Temperature. From the results, it

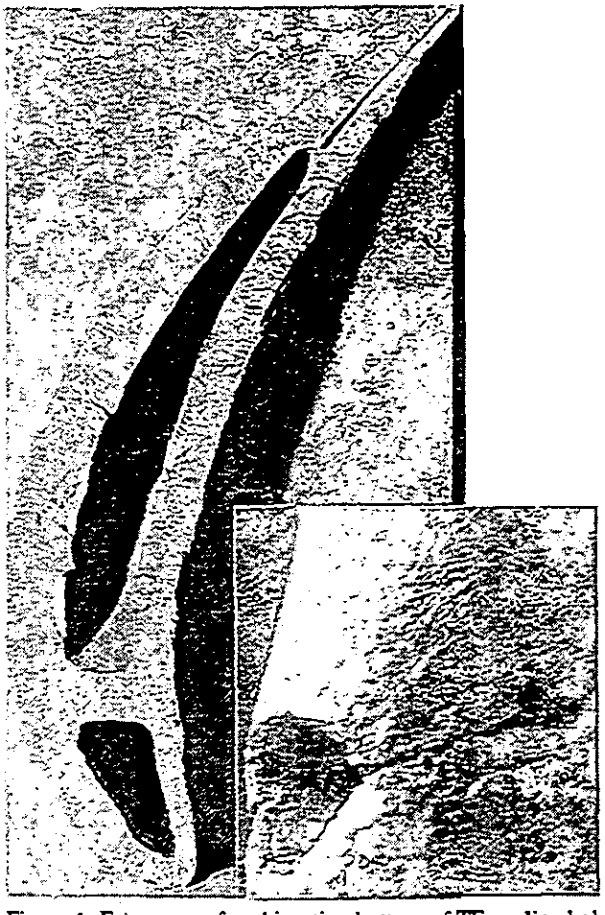

Figure 1. Fracture surface bisecting bottom of TE cooling hole (upper photograph) and cooling hole crack on another blade at 10X (lower photograph insert)

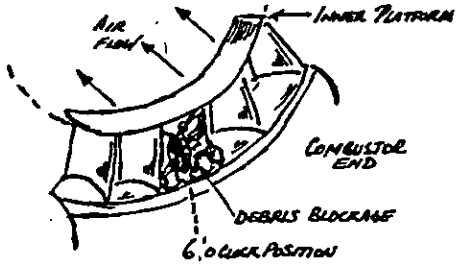

Figure 2. Sketch showing brick trapped in nozzle segment.

was evident that there was a degradation in compressor efficiency which was attributed to axial compressor fouling. This was not however a factor in the failure. In addition to basic performance trending, exhaust gas temperature (EGT) profiles and spreads were examined.

2.4.2 Exhaust Gas Temperature Profiles. A graphical plot was made of the EGT profile based on the eight exhaust temperature thermocouples and is presented in Figure 3. In general, the pattern held reasonably well except for an excursion in the data a few days prior to the failure. Of considerable significance was the fact that for two consecutive hours, thermocouple No. 6 exhibited a significant drop in temperature to 405 °C, when the expected value was 490°C.

With respect to the temperature spreads, an X-Y Scatter plot was created from log sheet data by plotting ($EGT_{Avg.}$ - $EGT_{min.}$)

[2]Because of the Air to Fuel ratios involved, 20 ppb of salt in the airflow is equivalent to 1 ppm in the fuel. Moreover, with the large air flow rate of this machine over 900 lb./sec, airborne salt ingestion is a very serious issue. Records of the fuel treatment indicated effective removal of salt.

on the abscissa and (EGT $_{Avg.}$ - EGT $_{max.}$) on the ordinate. This is shown in Figure 4. It is interesting to note that whereas all the data was within an "acceptable zone" defined by the OEM, there was a significant excursion on the day of the failure. All other data points were highly clustered around coordinates of (20,20).

This reinforces an important point pertaining to condition monitoring viz. step changes that occur in data are of significance even though absolute levels are quantitatively acceptable. The importance of trending and evaluating logsheet data is evident in this case.

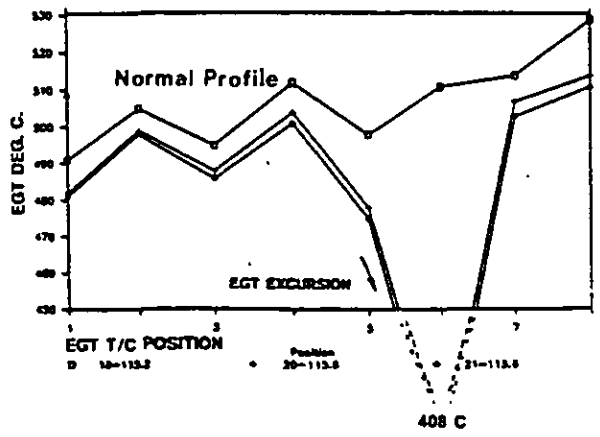

Figure 3. EGT Temperature profile excursion due to stator nozzle blockage.

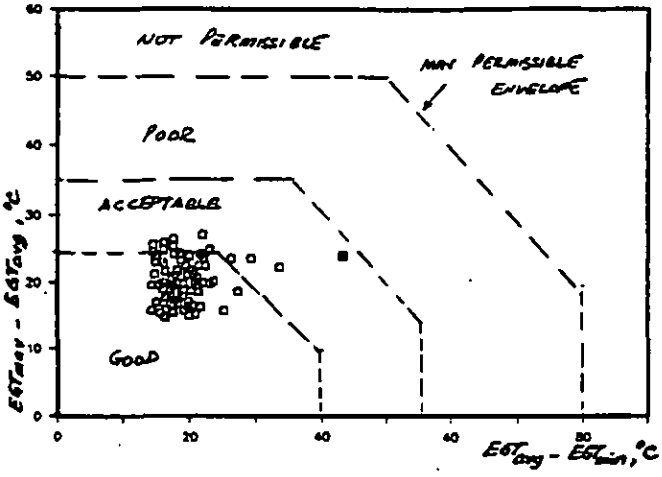

Figure 4. Excursion of Exhaust Temperature Spread.

2.4.3 Sulphidation. Based on visual observations and metallurgical analyses, sulphidation was an important contributing factor to the failure. Sulphidation can rapidly damage the base material and even a small loss of blade material can shift natural frequencies into dangerous regions causing resonance and high cycle fatigue. Sulphidation damage to the cooling holes would also result in localized overheating.

2.4.4 Study of Fuel Analysis Reports. Because sulphidation was a factor, possible modes of salt ingress were investigated. The liquid fuel system was first investigated. Data logs of fuel sample analysis were examined to check for the presence of metallic chemical elements harmful to the turbine and showed that contents of sodium, vanadium, and potassium were, on average, less than 0.1 ppm. Lead content was found less than 0.2 ppm. These concentrations were well within acceptable values and the evidence therefore pointed to airborne salt ingestion.

2.4.5 Blockage of the Nozzle Section and Its Effects on Blade Vibration. Observations made after the failure indicated that pieces of the combustor firebrick had lodged in the lower nozzle segment causing a blockage of approximately 80% (of that vane space). This occurred in the 6 O'clock position. It is possible that the blockage may have been far more severe in terms of percentage of nozzle area blocked prior to failure.

The effect of the blockage was to increase vibratory stresses on the blades resulting in abrupt loading/unloading as the blades traversed this position as shown in Figure 5. This situation is analogous to partial admission shock loading in a steam turbine. Due to the blockage, the localized Mach number and pressure drop affected rotating blade loads. It is difficult to analytically predict the effects of blockage as the severity would depend on the excitation magnitude and the damping associated with the excited mode. However, it is common knowledge that blockage of this nature can promote fatigue failures. Impulse harmonics and weakening of the blade due to sulphidation worked in unison to promote the failure.

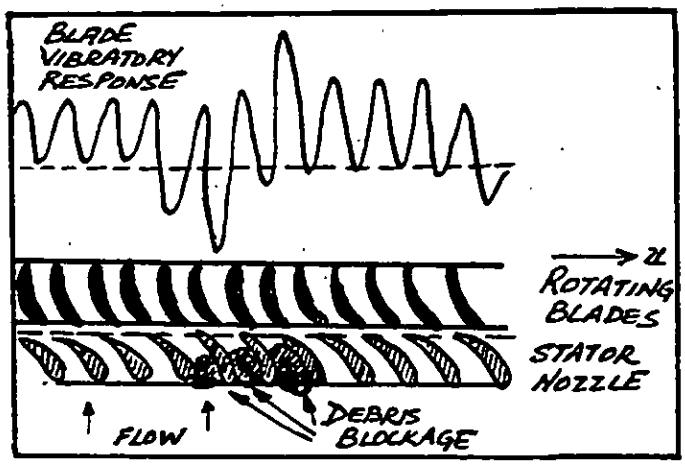

Figure 5. Increase in blade vibratory stresses due to blockage.

2.5 Case Summary.

The catastrophic damage experienced by the unit was initiated by 1st stage blade fatigue failure. There were several contributing factors. First, the increased vibratory stresses induced due to the blockage distortion caused unusually high alternating stresses. Second, sulphidation weakened the blade. The root cause was breakage of the firebrick from the combustor inner wall. This case illustrates the complicated interaction of operation, design, and environmental factors and underscores the importance of taking EGT deviations from the norm into account even when these are within an "acceptable region" in terms of absolute temperature spreads.

3.0 BLADE FAILURE OF AN AXIAL FLOW EXPANDER

3.1 Background.

This case involved multiple blading failures on a large single stage axial flow hot gas expander rated at 15 MW and operating at 3600 RPM with an inlet temperature of 1300°F (704°C) and a mass flow rate of 200 lb./sec (91 Kg/sec). The expander's availability was of utmost importance to the plant, and financial incentives for keeping the train operational were enormous. Impingement steam was used to cool the expander blades. The expander experienced four blade failures after installation.

3.1.1 First Blade Failure. The first failure occurred after approximately 3,000 hours of operation. Blades were found to be badly affected due to erosion caused by catalyst carryover. The base of the rotor blades had eroded due to steam impingement from the cooling nozzles (the steam flow for impingement cooling was 2,000 lb./hr (910 Kg/hr). The flow pattern on the blading indicated considerable turbulence near the base and at the leading edge at the tip section which might have excited the blades at operational speeds. It was felt that the rounding of the platform, as well as the cutting of the blade in such a uniform manner, could only have occurred from a steady impingement source.

3.1.2 Second Blade Failure. The second failure occurred 10 months later after 6,200 hours of operation. Blade notching and erosion had occurred at the base due to steam impingement. This was evident by the rounding effect on the blade platform. Catalyst had built-up on the shroud. The OEM felt that the failure was due to the bending stresses on the blade caused by the catalyst buildup on the shroud. The OEM also felt that the notch at the base was due to catalyst erosion. An alternate opinion was that the notch was caused by the steam injection and that that the failure resulted from the high stresses. A study of Larson-Miller parameters and Goodman diagrams was made for the blade material in order to determine whether a material change from Inconel 750 to Waspalloy should be made.

3.1.3 Third Blade Failure. The third failure occurred eight months after the second failure, after 5,500 hours of operation. The blade material was still Inconel 750 and the disk material Waspalloy. On the run leading to the third failure, steam flow was reduced from 2,000 to 1,000 lb./hr after 1850 hours of operation. Since a decision had been made to replace the blades, a reduction in steam flow was made to minimize the notching problems. When the unit was inspected, cracks were found on the fir tree upper section towards the trailing edge of the blades. The cracks indicated that high cycle fatigue (resonance induced) was a problem, however, the OEM attributed the cause to be due to insufficient cooling. Steam impingement effects were still evident at the leading edge of the blade near the base; but the magnitude was considerably less compared to the second failure. The reduced impingement damage, due to reduced steam cooling flow, confirmed that the problem was not one of catalyst carryover.

3.1.4 Fourth Blade Failure. The fourth failure occurred after an incremental 2,600 hours of operation approximately five months later. The blade material had been changed from Inconel to Waspalloy and the impingement cooling flow was reduced to 500 lb/hr. This blade failure occurred in the same region as in the third failure (top section of the fir tree); however, the location was on the leading edge of the blade. Electron microscope pictures indicated that a high cycle, low stress fatigue problem existed. Blade resonance conditions were suspected.

3.1.5 Candidate Causes. Based on a study of the four failures, the following candidate causes were considered:

1. Resonant frequency of the blade being excited at an "off-design" speed, about 2450 RPM, at which the unit was run for process reasons.
2. Resonant frequency of the blade being excited at design conditions due to process upset conditions or due to increased loading.
3. Poor choice of materials. Blade materials were Inconel 750 for the first three failures and Waspalloy for the fourth failure. Both materials have been used extensively in turbomachinery at much higher temperatures. Temperatures in the fir tree section of the rotor were estimated to be between 800-950°F (427-510 °C). Consequently, improper materials had a very low probability of being the underlying cause of the failure.

There was a high probability that the third and fourth failures were due to blade resonance and that temperatures may have contributed to the location of the failure position, (i.e., trailing edge for the third failure due to cooling being present at the leading edge and on the leading edge for the fourth failure due to absence of cooling). The main problem then was to ascertain whether the resonance occurred at the off-design speed range of 2,300-2,600 RPM or at the design speed of 3,600 RPM. Blade resonance was recorded by the OEM in a rap test and spectra indicated that resonances existed in multiples of 520 Hz and 590 Hz. Thus, at speeds of around 2,300-2,600 RPM, excitation modes (48E, 12E) could have led to blade resonance and ultimate failure. Blade resonance frequencies were in the 500 Hz - 2,000 Hz range, indicating that failure could occur in 1-6 hours of operation at these frequencies. In order to investigate the failures, a field test was planned.

3.2 Field Test.

The objective of this test was to locate the speed and excitation causing the resonance so as to try and avoid dangerous operational regimes. Air-cooled accelerometers were mounted on the expander mount trunion and bearings. Signals from the vibration transducers during startup, heating , loading cycles were recorded on an eight channel AM/FM magnetic tape recorder and analyzed using a real time spectrum analyzer.

3.3 Campbell Diagram And Modes Of Excitation.

Natural frequencies for the first flexural, torsional, axial and second flexural modes were between 540 and 2,133 Hz. Since material stiffness is reduced at operating temperatures, a "hot" and "cold" number was calculated. From the Campbell Diagram, it could be seen that excitation was induced by the number of blades (62E), as well as the stator (48E), the number of steam injection nozzles (9E), and the number of struts (8E). During the field test, the data was scanned for resonant peaks with particular attention being paid to conditions of: change in speed, temperature, load, and injection of cooling steam.

3.4 Interpretation Of Vibration Spectra.

The objective of the vibration spectrum analysis was to detect undesirable excitations, and to examine relative changes in amplitude that occurred at specific frequencies with changes in operation.

Figures 6(a) and 6(b) show the vibration response with and without steam injection. Blade passing frequencies exist on both spectra, however, blade resonant frequencies exist only in Figure 6(a), indicating that blades resonated as a result of steam injection. Figure 7 shows that as the steam flow is increased, there is an increase in excitation at frequencies of 980 Hz, 1442 Hz and 1978 Hz which are close to the natural frequencies.

The vibration analysis indicated two problems:

1. The excitation of blade resonance frequencies at speeds of 2,400-2,700 RPM. This implied that these speeds had to be avoided during operation. At other off-design speeds, the blade resonance was negligible.
2. Blade resonances were excited as a result of steam injection.

It is important to note that detection of blade excitation by the use of high frequency accelerometers is not always possible on turbomachinery. Success in this approach has also been documented by Parge(1990) and Mitchell (1975).

3.5 Recommendations & Results.

It was recommended that the expander be operated close to its design speed and flow. After a detailed study of blade material capability, a determination was made that steam injection provided minimal cooling benefits and was detrimental in terms of exciting blade resonances. A recommendation was made to discontinue the use of steam for blade cooling and to avoid operation in a particular speed zone. With these recommendations implemented and careful ongoing vibration monitoring program, an uninterrupted run of over 20,000 hours was achieved.

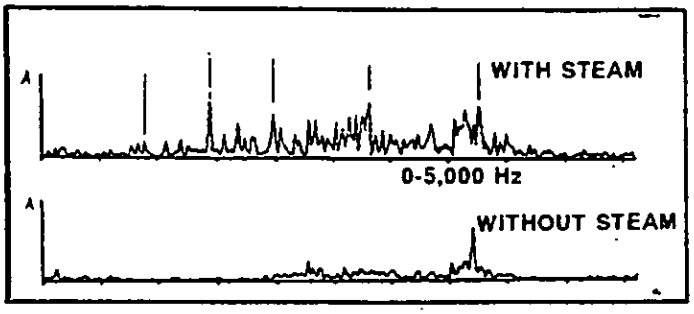

Figure 6. Vibration response with and without steam injection.

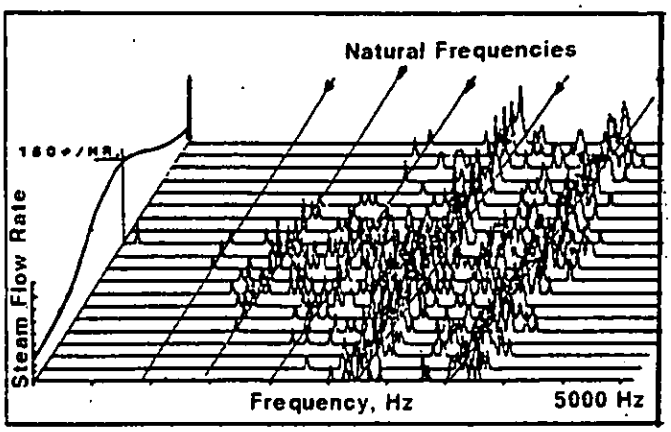

Figure 7. Accelerometer Based Vibration Cascade Showing Response with Steam Injection.

4.0 BLADE FAILURE OF A 15 MW PEAKING TURBINE

4.1 Background.

This case relates to a 1965 vintage 15 MW natural gas fired peaking gas turbine sited in the Gulf Coast region of the US. This case demonstrates how practical failure analysis and analytical work can complement each other.

The turbine was a single shaft (60Hz) unit with a flow rate of 270 Lb/Sec(123 Kg/Sec) and a pressure ratio of 7.5:1. The unit had a 19 stage compressor and a 7 stage turbine each being located in individual casings. The unit had run for approximately 29,000 hours with 2,410 starts when the failure occurred. On the day of the failure, operators reported high noise and vibration levels prior to the trip. After coast down, the rotor locked up. Substantial damage was found in the turbine section.

4.2 Description of the Failure.

Upon casing removal, the following turbine section damage was found:

1. One blade in the 4th stage had migrated and was found cocked axially. This blade was found to have suffered a total failure in the leading edge T-root section (both lands).
2. Severe damage was found in the 6th stage blading with two blades being found broken approximately 1.25" from the base. Fracture surfaces were typical of fatigue.
3. Severe blading damage was found in the 7th stage (DOD).
4. Vanes in row 6 and 7 were severely damaged (DOD)
5. Upon deblading and subsequent NDT inspection, it was found that cracks were present at the T-root sections of the 2nd through 5th stages blading.
6. The blade attachment regions in the drum type rotor indicated wear and corrosion, with the 1st and 7th stages being in the worst condition.

Figure 8 depicts the damage.

Figure 8. Broken blade lands(Upper photo) and standby corrosion damage to drum blade attachment region (Lower photo).

4.3 Metallurgical Analysis.

A metallurgical analysis of four blades was carried out. These included two 6th stage blades (fractured through the airfoil) and a 4th and 5th stage blade stage blade, which exhibited fluorescent penetrant indications on the blade attachment surfaces. The 4th stage blade had a chordwise crack on the airfoil, emanating from the trailing edge, 1½" above the platform.

4.3.1 Visual Observations. The 4th stage blade airfoil tip surface bore evidence of rubbing. This blade did not have a tip shroud or tie wire hole for vibration damping purposes. The airfoil was sectioned to open the chordwise crack which was 1.5 inches above the platform. The crack was caused by fatigue, with the origin being in or near the trailing edge.

The 6th stage blades examined had ruptured approximately 35mm and 60mm above the platform. The fractured surface on one of them was more heavily oxidized than the other, suggesting that one fracture preceded the other. The fracture surface on one blade was so badly oxidized that the typical fatigue crack clamshell markings were not detectable. The oxide coloration on the fracture surface of clearly showed that the fracture was caused by fatigue, originating in or near the trailing edge. Fretting damage was seen on the bearing surfaces of both blade attachments. Figure 9 shows the fatigue fracture surface.

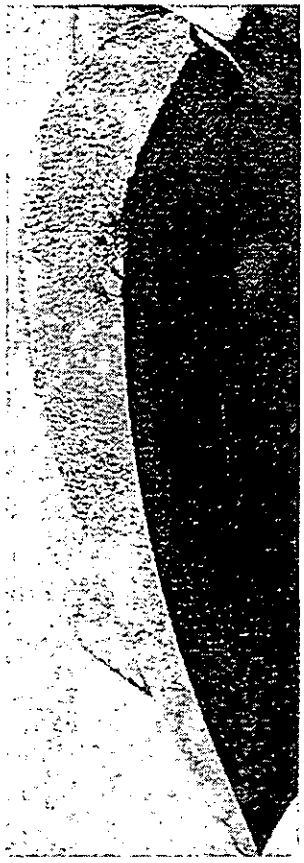

Figure 9. Fatigue fracture surface.

4.3.2 Metallographic Investigation. 4th, 5th and 6th stage blade microstructures were very similar, consisting primarily of austenite grains, similar to type 300 series stainless steels.

4.3.3 Hardness Investigation. Several 5 kilogram Vickers hardness impressions were made on each of the polished metallographic specimens. The 4th and 5th stage blade materials both averaged equivalent to HRC 16, while the 6th blade material averaged to HRC 24.

4.3.4 Scanning Electron Microscope (SEM) Investigation. Both of the 6th blade fracture surfaces were examined using a SEM but this examination did not yield any useful information about the origins of the fractures. The fractures from the 4th blade was also examined in the SEM. While no origin was found, some badly oxidized fatigue striations (i.e., "clamshell" markings) were noted.

In the case of the 4th blade airfoil fatigue crack, there were two considerations. First, the airfoil tip shroud *showed evidence of rubbing*; hence, this strumming may have set up resonant vibration in the airfoil, leading to the nucleation of the fatigue crack. Secondly, the alloy used for the 4th blade had a very low tensile strength. Since fatigue strength is directly linked to the ultimate tensile strength , it follows that fatigue crack initiation is relatively easy with a weak alloy.

4.4 Situation Analysis.

In order to troubleshoot the failure, the following analytical studies were conducted:

1. Review of forces on Blade attachments
2. Blade Stress analysis
3. Blade Natural Frequency analysis
4 Review of blading materials (UTS and Ni content)

4.4.1 Migration of the 4th Stage Blade and its Effect on Blade Vibration. The displaced 4th stage blade would induce a very high vibratory stress on the downstream blading due to the flow discontinuity effect. This was, in all probability, a major factor leading to fatigue failure in the 6th stage. The resulting flow discontinuity resulted in abrupt loading/unloading of the blades as they passed this position (analogous to partial admission shock loading). Due to blockage effect, the localized machine mach number and pressure drop changed, which in turn affected the loads imposed on the blading.

4.4.2 Fretting Damage in Blade Roots. Excessive vibration that occurred in the turbine, accelerated the process of fretting that caused the cracks found in almost all stage roots. The gas turbine hot section uses an internal groove double T- slot arrangement. In this type of design, the assembly is considerably "softer" in the circumferential direction. The circumferential component of the alternating bending forces has historically been a common cause of failure for the internal groove root. This type of root utilizes parallelogram shaped root platforms and is vulnerable to fatigue failures. The highest loading occurs on the top serration near the trailing edge and this is often responsible for inducing fatigue cracks in the adjacent fillet and shank corner.

Of the blades examined, 63% had cracks on the land trailing edge location where, as described above, the stresses are the highest. The blade bending moment is transferred to the rotor if the shank portion is tight in the rotor drum. (A drum type rotor assembly is relatively axially stiff. *If there is any looseness however, the load is transferred to the shank.* This load then adds to the existing centrifugal forces that exists and played a role in the 4th stage blade land failure.

Subsequent to the initial failure within the turbine, extended operation at exceedingly high vibration levels caused accelerated wear and fatigue on the blade land regions. Hittori et. al (1983), examined fretting fatigue in gas turbine disk/blade dovetail region under blade centrifugal and bending loads and showed that the amount of total slippage is very sensitive to the bending moment (i.e., alternating stress.)

Additionally, the blade disk interface provides an important source of damping[3] and this is most important for the lower vibration modes of the blade. Goodman and Klumpp (1956) have found that a highly beneficial reduction in resonant stresses can be achieved by friction damping. Several fatigue failures have typically originated by vibration at the lower modes.

4.4.3 Analytical Model for Root Section Stress. This analysis was conducted to get a feel for the operating stresses and to determine the design conservativeness of the blading. Dimensions were taken from the blading or scaled from drawings that were available. The approaches followed for the stress calculations were based on methods of Sohre(1975) and Dundas (1985). Several cases were studied to examine the sensitivity of blade stress to bearing area. The analysis pointed out relatively conservative stresses.

4.4.4 Evaluation of Vibratory Stresses. Figure 10 shows a Goodman Diagram created for the 3rd through the 7th stage blading. All of the stage materials have a UTS of approximately 100 KSI. The steady state stress was considered the sum of the gas bending stress and the centrifugal stress. The alternating stress is determined by applying a magnification factor of 3 to the gas bending stresses (Scalzo, 1991)

This has been designated as Case 1. The results have been shown plotted on a Goodman diagram. The results with a higher Magnification factor of 4.5 (Magnification Factor of 3 multiplied by a stress concentration factor of 1.5) is also shown in the diagram (Case 2). It is clear that both the 6th and 7th stages are close to design fatigue limit with factors of safety rapidly eroding as alternating stresses go up. The Goodman Factor of Safety dips below 1.5 (normally, the minimum acceptable) for the 6th and 7th

[3] Stick-slip friction damping.

stages. Thus, any loss of damping would result in a relatively rapid fatigue failure.

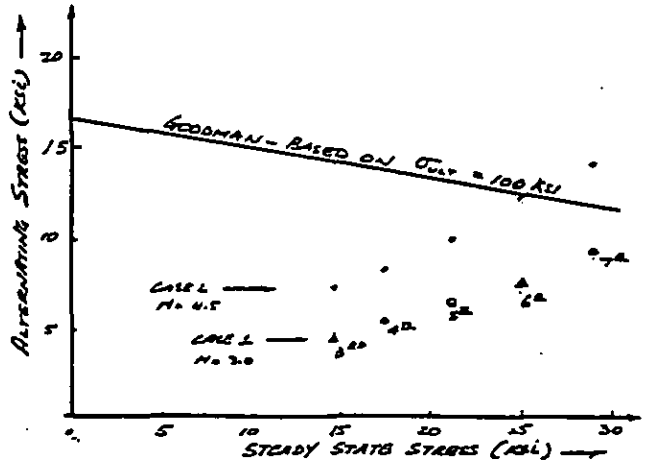

Figure 10. Goodman Diagram

4.4.5 Analytical Model for Evaluation of Blade Natural Frequencies. In order to obtain an estimate of blade natural frequencies, an analytical model along the lines suggested by Marscher (1985) was created to evaluate the bending mode (flap) mode of vibration. The analysis considered a free standing blade as a cantilever. The natural frequency calculated was corrected for centrifugal stiffening effects, blade camber , bow and taper. Operating temperatures were taken into account by means of reduction in Young's Modulus (E). The Young's Modulus values for austenitic steel were obtained from Faupel (1964). The effect of blade taper was neglected because taper ratios were relatively small for all stages and would induce a marginal effect on the natural frequency

The calculations showed that the 1st bending to operating speed ratio falls below 4 for the 7th stage blading. Common design practice requires that a margin of at least 4 be maintained. The 6th stage blade natural frequency could have easily been excited by the 4th order of the running speed caused by the displaced (cocked) blade which would cause flow distortion in the upstream stages. It is of critical importance to note that after the first 6th stage fatigue failure, there was a loss of integrity of the damping wire system. The 6th stage blading relied on frictional damping of the lacing wire to absorb vibration energy. With a loss in this damping, vibratory stresses increased by a factor of 3-4 times causing additional distress.

4.4.6 Blading Materials and Standby Corrosion. Another important factor that contributed to the problems was standby corrosion in the blade root attachment region. This is a problem that commonly afflicts peaking gas turbines. Corrosion products which accumulate in the blade attachment areas act as abrasives and increase clearances. In the presence of corrosives possibly from airborne salt, uncoated airfoils often develop corrosion pits which could progress into cracks.

4.5 Failure Scenario and Root Causes.

A combination of fretting wear and standby corrosion in the blade attachment areas caused looseness and a reduction in the blade bearing area which resulted in the total failure of the fourth stage blade land attachment area. The cocking of the 4th stage blade set up wakes ultimately resulting in the 6th stage blade fatigue failures. This case shows the interaction effects of environment (standby corrosion), design features and operating conditions. It also shows that considerable insight can be obtained by relatively simple modeling[4] techniques.

5.0 DOD BLADE FAILURE IN A 30 MW TURBINE

5.1 Background.

The subject gas turbine was a natural gas fired 30 MW single shaft, cold end drive, 3600 RPM unit that was in power generation service. The gas turbine operated at a turbine entry temperature of 850°C (1565°F) and with a compressor pressure ratio of 8:1. It had a 15 stage compressor, a single silo combustor and a 5 stage turbine. The gas turbine had operated for approximately 7 days at a load of 10 MW when it failed. The failure was preceded by a loud noise after which the turbine tripped on vibration. Vibration trip level were set at 40 microns, pk-pk.

Eighteen months prior to the failure which is the focus of this case study, a similar incident had occurred after which a new set of blades had been installed. The damage in this previous failure was of a FOD/DOD nature with severe damage occurring throughout the turbine section. The failure mode was impact overload with fracture surfaces being interdendritic in nature. Of particular importance, in this earlier failure, was that some small spherical particles were found adhered to the stator vane surface. At the time of the previous incident, the root cause for the DOD was not determined.

5.2 Description of the Failure.

All five (5) turbine stages were severely damaged with fracture damage being indicative of impact overload. The stator nozzles, the rotor blades, and drum were badly battered. Several blades from the first three stages had been cropped with the 3rd stage rotor blades being totally wiped out. Several blades in this row had broken at the root near the cooling hole. The compressor section and bearings were not damaged. A few compressor stages indicated tip rubs probably caused by the tremendous unbalance forces that resulted with loss of turbine blading. The rubs occurred at the center of the rotor where deflection would be the greatest. The turbine section was totally destroyed and is shown in Figure 11 .

5.2.1 Debris in Turbine Careful examination of the debris in the turbine section revealed what appeared to be a foreign object located in the lower stator case before the 4th stage stator vanes. This piece shown in Figure 12 was badly battered, was approximately 40 mm long and had a diameter ranging between 15 -20 mm and did not look like a turbine section component. Thereafter, the combustor dome was inspected. The dome had six (6) struts to hold the swirl vane support inner ring which were held by clevis pins approximately 55 mm in length and a diameter of 20 mm. These clevis pins held the strut and were then locked in place by cotter pins. Two of the six struts had missing clevis pins. The ingestion of these clevis pins was the cause of the domestic object damage in the turbine section. Figure 13 shows details of the construction of the silo combustor and shows the locations of the missing pins.

5.3 Metallurgical Analysis.

5.3.1 Details of the Examination. Several components including blades, stator blades and other clevis pins from the combustor were selected for metallurgical examination.

Clevis Pins. Some of the clevis pins had cotter pins installed that were magnetic and made from relatively large cross-section wire,

[4] While there are several cases where Finite Element Models are appropriate, it is the authors contention that simple hand (or spreadsheet) calculations can provide a quick engineering feel of the blade dynamics for use in field troubleshooting situations.

while one cotter pin was non-magnetic and was made from a much smaller cross-section wire. Significant fretting corrosion

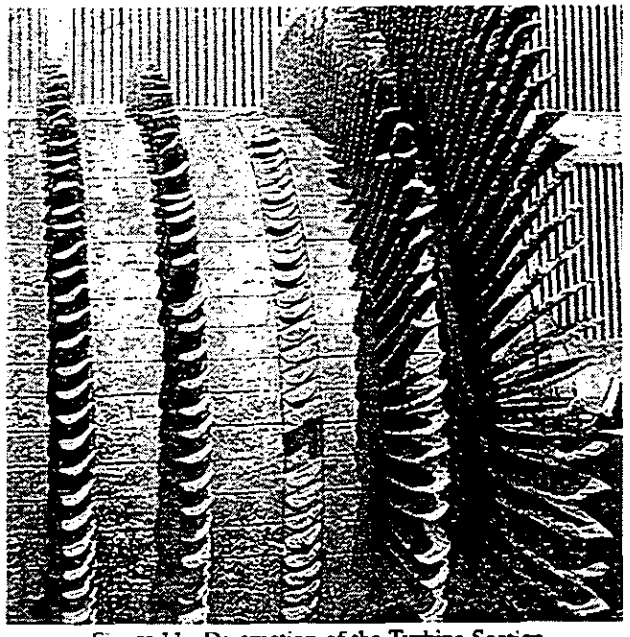

Figure 11. Destruction of the Turbine Section.

Figure 12. Pin found in turbine debris.

damage was noted where the cotter pins protruded from both ends of the cross drilled holes - the most serious being on the thin, non-magnetic cotter pin. The battered piece found in the turbine debris and the clevis pin samples exhibited substantially the same micro-structures.

Stators and Blades. All of the fracture surfaces were 100% interdendritic in nature. No evidence of creep, stress rupture, or fatigue cracking was observed. All other non-fracture damage (i.e., indentation, smearing, bending, "machining") were considered consistent with overall turbine damage.

Overtemperature Analysis. A standard over temperature examination was done on one of the 1st stage stators, comparing the micro structure at the midspan, leading edge position on the airfoil with that from a region outside of the gas path, as a baseline. No evidence of gamma prime precipitate solutioning, (the accepted indicator of service over temperature of nickel-based superalloys) was observed.

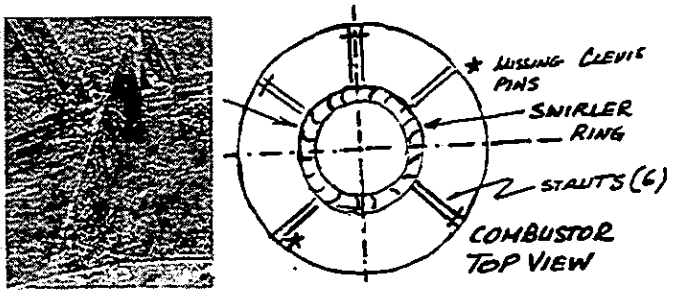

Figure 13. Missing clevis pin.

5.4 Clevis Pin Transport Model.

A simple model was created to examine the transport of the clevis pin in the U-duct and into the turbine. This model evaluated the capability of the air stream to lift the pin vertically into the air stream up the U duct and into the nozzle section. The transport probably occurred along the duct surface and the pin then was ingested into the turbine in a lengthwise orientation. The model considered the following parameters:

Pin Length 5.5 cm, diameter 1.75 cm
Material density = 0.283 lb_m/in^3
Coefficient of Drag = 0.7–0.8 (Cylindrical pin with L/D ≈ 5)
Gas Temperature = 1565°F (2025°R)
Pressure = 116 psia (Pr. Ratio of 7.85:1 assumed[5])
Pin Projected area = 1.45 in^2
The governing equation is,

$$\text{Lift} = C_d A \rho V^2/2 \qquad (1)$$

where, C_d is the Coefficient of drag, A the cylinder projected area, ρ the air density in slugs and V the airflow Velocity. This equation was used to determine the ability of the airflow to transport the pin to the turbine nozzle vanes. Even at an air velocity of 50 ft/sec, a 1.3 lb pin could be lifted. The new pin was estimated to weigh no more than 0.25 lbs.

5.5 Case Summary

The massive turbine failure was the result of ingestion of a clevis pin, which had been liberated from the top of the silo combustor. The dislodging was the result of fretting damage, which disintegrated a cotter pin, used for retention of the clevis pin. In the light of this finding, it is entirely possible that the earlier failure, was also caused by the liberation of a clevis pin from the top end of the silo burner. The low alloy steel globules on the 1st stage stator airfoil surface found during the first failure metallurgical study were definitely low alloy steel, and in all likelihood were derived from an ingested clevis pin. This case stresses the importance of a thorough search of debris for telltale clues.

[5] As the machine was operating at part load (10 MW), the Pressure ratio and firing temperature were probably lower than the assumptions in this model. Yet, for estimation purposes, these numbers provide a feel for the situation.

7.0 IMPORTANCE OF FUEL SYSTEM FUEL QUALITY

7.1 Background.

This case involved a single shaft dual fuel heavy duty gas turbine rated at 18 MW that had operated for 13,000 hours. The failure occurred during a changeover from natural gas to liquid fuel when the unit output dropped from 18 MW to 8 MW. The operator initiated a change back to No. 2 fuel oil and turbine tripped on high exhaust gas temperature.

7.2 Damage to Gas Turbine and Site Inspection.

Due to internal damage to the gas turbine, the rotor had moved over ½" in the axial direction causing damage on the aft end of the first stage turbine wheel. A significant finding was that the fuel gas tip of one of the combustors had come loose and was found lodged in the combustion liner.

The first stage nozzle directly opposite the combustor can that had the loose gas tip was burnt away. The nozzle support ring was also severely damaged. The second stage nozzle showed some signs of over temperature but the predominant damage was due to Domestic Object Damage. The first stage blades showed signs of over temperature and burned portions at the base of the blade characteristic of liquid carryover. The blade tips were broken off. Due to the axial movement of the rotor, the axial compressor had rubbed..

7.3 Situation Analysis.

7.3.1 Gas Overfueling Without the Presence of Hydrocarbon Liquids. As the nozzle cap unscrewed, there was an increase in the gas flow rate to the combustor. Calculations by the OEM indicated an increase in flow of about 2-9 times the normal quantity. (This would have caused a consequent reduction in flow to the other combustors). With an increase in fuel flow, the Fuel/Air (F/A) ratio exceeded the upper limit of flammability causing the flame to move downstream of the reaction zone. The flame would re-establish itself at a location where there was extra air and some vorticity to slow down part of the flow, for example, at the main dilution holes. At some intermediate stage, it is possible that a long streak of flame could have overheated the liner and transition piece. Corner vortices set up in the transition piece could also act as flameholders. It was also possible that the nozzle vanes themselves acted as flame holders.

7.3.2 Effect of Liquid Hydrocarbon in Gas. If a liquid was present in the gas supply, then, as the nozzle cap became loose, liquid would tend to be transported to the faulty combustor. If a significant quantity of liquid was transported in this manner, through a reaction zone where gas overfuelling had caused the flame to move through a reaction zone (downstream), droplets would impinge on the inner partition ring. Influenced by the secondary flow system, the liquid would tend to accumulate against the convex face of the vane and the enhanced flame would attack the partition ring.

7.4 Discussion

This case shows how severe blading failure can be caused by design weaknesses (loosening of the burner tip) not directly related to the blading. The fuel nozzle problem was solved by the use of a strap welded to the body and cap and by the use of lockwire. Furthermore, the case stresses the importance of good fuel quality and effective EGT monitoring.

8.0 SUMMARY

Blading failures in gas turbines account for a major proportion of serious outages. Troubleshooting and resolution of complex blading failure problems call for an interdisciplinary engineering effort to ensure that repeat failures do not occur upon startup of the machine. Finding the underlying cause can be difficult, but is essential. Failures must be examined, not only from a metallurgical perspective, but also from a design, operation and maintenance standpoints. Investigations have to identify root causes and contributing factors. The ultimate goal is, however, to recommend and institute changes in design, operation or maintenance procedures to ensure that problems do not recurr. Several case studies have been presented to consolidate the treatment of blading failure as presented in Parts A, B, & C of this paper and to illustrate the process of troubleshooting blade failures.

REFERENCES

Allianz (1978), "Handbook of Loss Prevention", Springer Verlag, NY, 1978

Armstrong, E.K., and Stevenson, M.A.,(1960) "Some Practical Aspects of Compressor Blade Vibration", J. of the Royal Aeronautical Society, Volume 64, No. 591, March 1960, pp 118-130.

Dundas, R.E.(1993a) "Investigation of Failures in Gas Turbines" Part 1 - Techniques and Principles of Failure Investigation", ASME International Gas Turbine and Aeroengine Congress, Cincinnati, May 24-27, 1993 ASME Paper No: 93-GT-83.

Dundas, R.E.(1993b) "Investigation of Failures in Gas Turbines" Part 2 - Engineering and Metallographic Aspects of Failure Investigation", ASME International Gas Turbine and Aeroengine Congress, Cincinnati, May 24-27, 1993 ASME Paper No: 93-GT-84.

Dundas, R.E., (1985) "Mechanical Design of the Gas Turbine", Sawyer's Gas Turbine Engineering Handbook, Vol I, 3rd Edition, Ed. Sawyer, J.W., Turbomachinery International Publications, 1985.

Dundas, R.E., Japikse, D., (1985) "Preliminary Design of the Gas Turbine", Sawyer's Gas Turbine Engineering Handbook, Volume I, 3rd Edition, Ed. Sawyer, J.W., Turbomachinery International Publications, 1985.

Faupel, J.H.,(1964) "Engineering Design," J.H. Wiley, 1964

Goodman, L.E., Klump, J.H., (1956), "Analysis of Slip Damping with Reference to Turbine Blade Vibration," Journal of Applied Mechanics, Transactions of the ASME, Vol 23, No 3, Sept 1956.

Hitori, T., Sakata, S., Ohnishi, H., (1983), "Slipping Behavior and Fretting Fatigue in the Disk/Blade Dovetail Region.", International Gas Turbine Congress, Tokyo, October 1983, Paper No: 83-TOKYO-IGTC-122.

Marscher, W.D.,(1985) "Structural Design and Analysis", Sawyers Gas Turbine Handbook, Vol I, Turbomachinery International, 1985

Meher-Homji, C.B., (1995A), "Blading Vibration and Failures in Gas Turbines: Part A- Blading Dynamics and the Operating Environment", 40th ASME Gas Turbine and Aeroengine Congress, Houston, TX, June 5-8, 1995.

Meher-Homji, C.B., (1995B), "Blading Vibration and Failures in Gas Turbines: Part B-Compressor and Turbine Airfoil Distress", 40th ASME Gas Turbine and Aeroengine Congress, Houston, TX, June 5-8, 1995.

Meher-Homji, C.B., (1995C), "Blading Vibration and Failures in Gas Turbines: Part C-Detection and Troubleshooting", 40th ASME Gas Turbine and Aeroengine Congress, Houston, TX, June 5-8, 1995.

Mitchell, J., (1975), "Examination of Pump Cavitation, Gear Mesh and Blade Performance Using External Vibration Characteristics," Proceedings of the 4th Turbomachinery Symposium, Texas A&M University, October 14-16, 1975, pp 39-45.

Parge, P.(1990), "Non-Intrusive Vibration Monitoring for Turbine Blade Reliability", Proceedings of the Second International Machinery Monitoring and Diagnostic Conference, October 22-25, 1990, Las Angeles, California, pp 435-446

Passey, R.D.C., (1976), "Reliability of Compressor Airfoils," Prog. Aerospace Science, Vol 17, 1976, pp 67-92.

Scalzo, A.J., (1991), "High-Cycle Fatigue Design Evolution and Experience of Freestanding Combustion Turbine Blades," International Gas Turbine and Aeroengine Congress, Orlando, Florida, June 3-6, 1991, ASME Paper No:91-GT-13

Sohre, J.S.,(1975) "Steam Turbine Blade Failures, Causes and Corrections", Proc. of the 4th Turbomachinery Symposium, Texas A&M University, College Station, TX, October 1975.

Acknowledgments.

The author wishes to acknowledge the contributions of Feroze J. Meher-Homji, PE. Chief Engineer (Mechanical), BEI for his invaluable help and technical advice in preparing this paper. Most of the metallurgical work was done by I.W. Glater, PE, CSP.